Electr Eng (2018) 100:913–933
https://doi.org/10.1007/s00202-017-0539-x

ORIGINAL PAPER

A new interactive sine cosine algorithm for loading margin stability improvement under contingency

Belkacem Mahdad[1] · **K. Srairi**[1]

Received: 15 August 2016 / Accepted: 29 April 2017 / Published online: 17 May 2017

Abstract In this paper, a new method called *sine cosine algorithm* is adapted in coordination with an interactive process to improve the power system security considering loading margin stability and faults at specified important branches. In this study, the loading margin stability is optimized in coordination with total cost, total power loss, total voltage deviation and voltage stability index. In order to locate the best loading margin stability, an initial global database containing suboptimized control variables is generated based on two indices named global and local critical reactive margin security related to generating units. The optimized loading margin stability is improved in coordination with the availability of reactive power of different shunt FACTS devices installed at particular locations. The robustness of the proposed planning strategy is validated on a small test system, the IEEE 30-Bus and to a large test system, the IEEE 118-Bus. Optimized results found confirmed clearly the improvement of loading margin stability at critical situations such as faults at specified branches.

Keywords Loading margin stability · Security OPF · Contingency · Metaheuristic methods · Sine cosine algorithm · Shunt FACTS · Critical reactive margin stability

1 Introduction

Due to limitation in production resources related to economical aspect and environmental constraints, transmission systems are forced to operate very close to their security limits. Statistical researches clearly confirmed that the majority of blackout occurred in the world lies on critical situations such as load growth and faults at important transmission lines. Ensuring flexible and optimal equilibrium between energy production and consummation under severe disturbances such as load growth and faults is a challenge to experts and industrials. Since the simplified economic dispatch introduced by Carpentier [1], a large number of projects and researches have been developed to solve the original formulation of optimal power flow [2]. In the literature, various mathematical methods have been applied to solve the simplified OPF [2–7]. As well confirmed by the majority of researches, the determinist methods rely on some simplification assumptions such as initial condition, convexity of objective function, continuity and differentiability fail to achieve the global solution in particular when practical constraints related to generating units such as valve-point effect, multi-fuel and prohibited zones and also by considering critical situations such as load growth and cascade contingencies. The actual OPF problem known as security OPF is an important subproblem of modern power system planning and control. Security OPF consists in optimizing one or multi-particular objective functions by adjusting a set of continuous and discrete control variables under critical situations such as load growth and contingency, while satisfying operation and security constraints [8]. The extensive necessity to solve practical problems related to power system operation and control and to overcome the drawbacks of the traditional methods, an efficient category of global optimization methods called metaheuristics has been developed and proposed in a large number of papers to solve several problems related to modern power system operation and control [9,10]. In [11], a novel algorithm inspired from the gray wolf behavior is proposed to solve various optimization problems. In order to enhance the performances of the recent original GWO

✉ Belkacem Mahdad
bemahdad@yahoo.fr

[1] Department of Electrical Engineering, University of Biskra, Biskra, Algeria

algorithm in solving practical OPF considering loading margin stability and contingency, a flexible planning strategy adapted with GWO algorithm is proposed in [12] to solve Blackout risk prevention in a smart grid, in [13], also the concept of gray wolf optimizer is adapted and applied for solving the optimal reactive power dispatch problem, in [14] a new hybrid method based on the combination between PSO and multi-verse optimizer named (HPSO-MVO) is proposed and applied to solve the reactive power planning. The main idea introduced is that the PSO technique used for exploitation phase and MVO for exploration phase which allows creating flexible balance between the two phases to achieve the near global solution, in [15] a modified bacteria foraging algorithm is adapted and applied for solving the security-constrained optimal power flow considering both the wind sources and conventional thermal generation, and in [16] a hybrid method called Fuzzy harmony search algorithm is proposed and applied to solve security OPF problems, a Fuzzy logic system (FLS) is adapted to adjust dynamically the pitch rate (PR) and bandwidth rate of the original Harmony search algorithm, the performances of the combined method have been improved compared to the standard Harmony search algorithm, in [17] a new adaptive partitioning flower pollination algorithm (AFPA) was applied to solve the security-constrained optimal power flow, the new adaptive mechanism search based on adjusting dynamically particular parameters of the FPA is proposed to enhance the performances of the original FPA in terms of solution quality and maximum number of generation and trials required, in [18] a supervised firefly algorithm is applied for optimal placement and sizing of voltage controlled distributed generators in unbalanced distribution networks, in [19] a new symbiotic organisms search algorithm is applied for solving the optimal power flow problem considering practical constraints such as valve-point effect and prohibited zones, in [20] a differential search algorithm is proposed for solving multi-objective optimal power flow problem, in [21], a novel Moth Swarm Algorithm (MSA), inspired by the orientation of moths toward moon light, is adapted and applied to solve constrained OPF problem, the particularity of the proposed variant based on association of learning mechanism with immediate memory and population diversity crossover for Lévy-mutation is to establish a tradeoff between the exploitation and exploration during search process. In [22], and in order to improve performances of the standard PSO by well balancing between exploration and exploitation search process to achieve the near global optimum, a new variant-based PSO named particle swarm optimization with an aging leader and challengers algorithm was adapted for solving the OPF, in [23] a contingency partitioning approach for preventive-corrective security-constrained optimal power flow computation is proposed, in [24] an adaptive real-coded biogeography-based optimization is applied for solving the optimal power flow for a deregulated power system, in [25], a combined method based on particle swarm optimization and gravitational search algorithm (PSOGSA) is efficiently adapted and applied to solve the optimal reactive power dispatch. The main particularity of the proposed hybrid method is that the GSA designed to achieve the exploration phase, and PSO adapted to achieve the exploitation phase, in [26] a parallel metaheuristics method for graphics processing units is successfully applied for solving the large OPF, the robustness of this parallel optimization technique validated on two large test systems IEEE 118-Bus and IEEE 300-Bus and will be considered as a useful and a competitive tool to solve various practical power system planning for large test systems.

From the review and statistical analysis of the different global optimization methods cited in the recent literature which applied to solve the security OPF problems, we can conclude that the main particularities of these methods in terms of solution quality and convergence characteristics are summarized as follows:

- A number of new methods and developed variants-based standard metaheuristics methods have been investigated in how to choose and adjust the best initial parameters to achieve the near global solution.
- In special complex optimization cases with various objective functions, the dynamic adjustment of parameters is not sufficient to achieve the best solution, in such situations, the hybridization concept is introduced to maintain flexible interaction between exploration and exploitation during search process to achieve the near global solutions.
- For solving large power systems with accuracy, the concept of parallelism is also investigated in many papers. The parallel execution of multi-subsystems enhances the solution quality and reduces the execution time in particular in solving large practical power systems.

We can conclude that, due to the complexity of the practical power system planning problems, characterized by the nonlinearity of objective functions and constraints, there is no à generalized method can be considered as a standard tool in solving all optimization problems related to power system planning operation and control. Therefore, recently there is huge number of novel algorithms proposed to solve various optimization problems. One of the very recently developed optimization techniques is the sine cosine algorithm (SCA) which is a population-based optimization algorithm introduced by Mirjalili [27] for solving several real optimization problems. The performances of the SCA have been well demonstrated on a set of well-known test cases including unimodal, multi-modal, and composite functions [27]. The main particularity of the SCA is related to its simplicity in programming and its ability to maintain a flexible balance between exploration and exploitation during search process.

In this paper, a new planning power system strategy implemented within a new interactive variant-based SCA is proposed to improve the solution of security OPF under critical situations such as loading margin stability and contingency. The novelty and contributions of this paper can be outlined as follows:

- Two indices named critical reactive margin stability and global critical reactive margin stability are proposed to find the first initial feasible solution.
- The loading margin stability is an important index for blackout prevention strategy of practical power system. A new power system planning strategy based on reactive margin stability index is implemented within the SCA to improve the margin loading stability considering contingency.
- A parallel execution of the SCA based on three practical candidate initial solutions is proposed.
- During search process, three control parameters $r1$, $r2$, and $r3$ are dynamically adjusted to overcome the premature convergence.
- The proposed power system planning strategy is capable of finding a competitive solution of margin loading stability in coordination with various objective functions such as voltage deviation, total power loss and voltage stability.

The performances of the proposed new variant-based SCA are tested and validated on two practical test systems, the IEEE 30-Bus and the IEEE 118-Bus considering various objective functions such as minimization of fuel cost, voltage deviation, total power loss, and total voltage stability. These objective functions are optimized at normal condition and under critical situations such as loading margin stability and contingency.

2 Multi-objective optimal power flow

The multi-objective OPF is an important subproblem of power system planning and control. It consists of optimization of one or a combination of many objective functions by adjusting the setting of control variables, while satisfying several equality and inequality constraints [12]. In general form, the mathematical formulation of the standard multi-objective OPF problem is given as follows:

$$\text{Minimize } J_i(x,u) \quad i = 1,\ldots,N_{\text{obj}} \tag{1}$$

$$\text{Subject to: } g(x,u) = 0 \tag{2}$$

$$h(x,u) \leq 0 \tag{3}$$

where J_i is the ith objective function, and N_{obj} is the number of objective functions, g and h are the equality and inequality constraints, related to power balance and power system security. The vector of state and control variables are denoted by x and u, respectively.

1. State variables

In general, the state vector variable is expressed as:

$$x = \left[\delta, V_{\text{L}}, P_{\text{Gs}}, Q_{\text{g}}\right]^{\text{T}} \tag{4}$$

The state variable composed by:

Load bus voltage angles δ, load bus voltage magnitudes V_{L}, slack bus real power generation P_{Gs}, and generator reactive power Q_{g}.

2. Control variables

The vector control variable is expressed by:

$$u = \left[P_{\text{g}}, V_{\text{g}}, B_{\text{sh}}, B_{\text{svc}}, t\right]^{\text{T}} \tag{5}$$

The control variables consist of:

Real power generation P_{g}, generator terminal voltage V_{g}, shunt capacitors/reactors B_{sh}, shunt dynamic compensators (SVC) B_{svc}, and transformers tap ratio t.

2.1 Constraints

1. Equality constraints

In general, the equality constraints $g(x)$ represent the balance between production and consummation. The real and reactive power balance equations are expressed by the two generalized equations:

$$P_{\text{g}i} - P_{\text{d}i} - V_i \sum_{j=1}^{N} V_j \left(g_{ij}\cos\delta_{ij} + b_{ij}\sin\delta_{ij}\right) = 0 \tag{6}$$

$$Q_{\text{g}i} - Q_{\text{d}i} - V_i \sum_{j=1}^{N} V_j \left(g_{ij}\sin\delta_{ij} - b_{ij}\cos\delta_{ij}\right) = 0 \tag{7}$$

where N is the number of buses, $P_{\text{g}i}$, $Q_{\text{g}i}$ are the active and the reactive power generation at bus i; $P_{\text{d}i}$, $Q_{\text{d}i}$ are the real and the reactive power demand at bus i; V_i, V_j, the voltage magnitude at bus i, j, respectively; δ_{ij} is the phase angle difference between bus i and bus j, respectively, g_{ij} and b_{ij} are the real and imaginary parts of the admittance (Y_{ij}).

2. Inequality constraints

In general, the inequality constraints are associated with reliable operation of all elements of power system, and reflect

the security limits associated with sate and control variables organized as follows:

$$V_{gi}^{\min} \le V_{gi} \le V_{gi}^{\max}, \quad i = 1, 2, \ldots, Npv \tag{8}$$

$$P_{gi}^{\min} \le P_{gi} \le P_{gi}^{\max}, \quad i = 1, 2, \ldots, Npv \tag{9}$$

$$Q_{gi}^{\min} \le Q_{gi} \le Q_{gi}^{\max}, \quad i = 1, 2, \ldots, Npv \tag{10}$$

$$t_i^{\min} \le t_i \le t_i^{\max}, \quad i = 1, 2, \quad , Nt \tag{11}$$

$$B_{\text{SVC}}^{\min} \le B_{\text{SVC}} \le B_{\text{SVC}}^{\max} \tag{12}$$

$$V_{\text{L}i}^{\min} \le V_{\text{L}i} \le V_{\text{L}i}^{\max}, \quad i = 1, 2, \ldots, Npq \tag{13}$$

$$S_{\text{l}i} \le S_{\text{l}i}^{\max}, \quad i = 1, 2, \ldots, Nbr \tag{14}$$

where $V_{gi}^{\min}$, $V_{gi}^{\max}$ are the limits on the generator bus voltage magnitude, $P_{gi}^{\min}$, $P_{gi}^{\max}$ are the limits on the output of active power generation, $Q_{gi}^{\min}$, $Q_{gi}^{\max}$ are the limits on the output of reactive power generation, $t_i^{\min}$, $t_i^{\max}$ are the limits on the tap ratio (t) of transformer, $B_{SVC}^{\min}$, $B_{\text{SVC}}^{\max}$ are upper and lower susceptance limits of shunt SVC Controllers, $V_{\text{L}i}^{\min}$, $V_{\text{L}i}^{\max}$ are the limits on voltage magnitude at loading buses (*PQ bus*) and $S_{\text{l}i}^{\max}$ is the maximum transmission line loading.

2.2 Objective functions

In the literature, many objective functions have been used by researchers to evaluate and improve the performances of practical power systems. These objective functions may be optimized individually and simultaneously.

1. Minimization of total cost

The total fuel cost is the most objective functions largely considered in security OPF studies. The quadratic form is the simple model which is formulated using the following equation:

$$J_1(x, u) = \sum_{i=1}^{\text{NG}} \left(a_i + b_i P_{\text{g}i} + c_i P_{\text{g}i}^2 \right) \tag{15}$$

where NG is the number of thermal units, P_{gi} is the active power generation at unit i, and a_i, b_i and c_i are the cost coefficients of the ith generator that reflect the quadratic form.

2. Minimization of voltage deviation

The total voltage deviation is optimized by minimizing the following objective function:

$$\text{VD} = \sum_{i \in \text{NL}} |V_i - V_{\text{ref}}| \tag{16}$$

$$J_2(x, u) = \text{VD} + \text{Penalty} \tag{17}$$

where V_{ref} is the desired voltage at all load buses, in general taken equal to 1 p.u.

3. Minimization of voltage stability index

Voltage stability index firstly introduced by Kessel and Glavitch [28] becomes an important index to electric utility. The developed index named *L-index* is based on the feasibility of power flow equations for each node. The *L-index* of a bus indicates the proximity of voltage collapse condition of that bus. It varies between 0 and 1 corresponding to no load and voltage collapse, respectively.

The objective function related to voltage stability can be expressed as follows:

$$L_{\max} = \max\left(L_j\right) \quad j = 1, 2, \ldots, N_L \tag{18}$$

where L_j denotes the individual L-index of bus j.

Therefore, in order to simultaneously minimize the total fuel cost in coordination with total voltage stability represented by $L_{\max}$, the two objective functions are combined as follows:

$$J_3(x, u) = \sum_{i=1}^{\text{NG}} \left(a_i + b_i P_{\text{g}i} + c_i P_{\text{g}i}^2 \right) + \lambda_{L\max} \times L_{\max} \tag{19}$$

where $\lambda_{L\max}$ is a weighting factor, determined by experience to balance between the two objective functions.

4. Minimization of a combined voltage deviation and cost

In order to simultaneously minimize the voltage deviation in coordination with total fuel cost, the following combined equation is proposed:

$$J_4(x, u) = \sum_{i=1}^{\text{NG}} \left(a_i + b_i P_{\text{g}i} + c_i P_{\text{g}i}^2 \right) + \lambda_{\text{VD}} \times \text{VD} \tag{20}$$

where λ_{VD} is a scaling factor chosen to balance between the two objective functions.

5. Minimization of total power losses

The total active power loss is optimized by minimization the following objective function:

$$P_{\text{loss}} = \sum_{k=1}^{N_l} g_k \left[(t_k V_i)^2 + V_j^2 - 2 t_k V_i V_j \cos \delta_{ij} \right] \tag{21}$$

$$J_5(x, u) = P_{\text{loss}} + \text{Penalty} \tag{22}$$

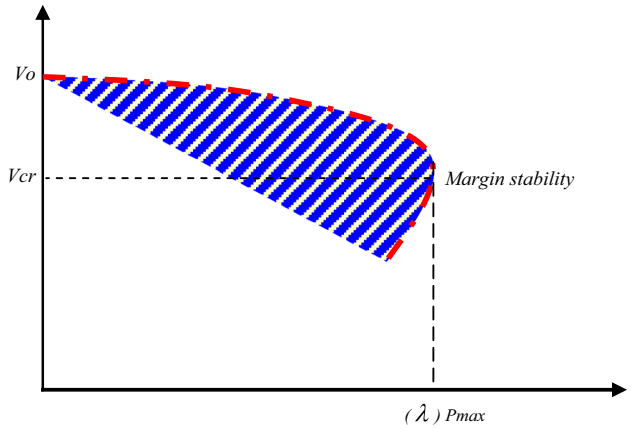

Fig. 1 Loading margin stability

6. Minimization of a combined total power loss and cost

In order to simultaneously minimize the total power loss in coordination with total fuel cost, the following combined equation is proposed:

$$J_6(x,u) = \sum_{i=1}^{\mathrm{NG}} \left(a_i + b_i P_{gi} + c_i P_{gi}^2\right) + \lambda_{pl} \times P_{\mathrm{loss}} \tag{23}$$

where λ_{pl} is a scaling factor chosen to balance between the two objective functions.

7. Maximization of loading margin stability

The loading margin stability is an important index which reflects the ability of the system to deliver dynamically power to consumer under critical situations [12]. As a result and to ensure the security of practical power system under load growth, the loading margin stability is optimized considering various objective functions such as, the total voltage deviation and the total power loss. The schematic representation of loading margin stability is shown in Fig. 1. The following equations describe the loading margin stability index.

$$P_{\mathrm{new}} = \lambda \cdot P_{\mathrm{base}} \tag{24}$$

$$Q_{\mathrm{new}} = \lambda \cdot Q_{\mathrm{base}} \tag{25}$$

where P_{new}, P_{base}: the new and base active power demands

$$J_7(x,u) = \mathrm{Max}\,(\lambda) \tag{26}$$

Q_{new}, Q_{base}: the new and base reactive power demands.

8. Maximization of loading margin stability and total power loss

The loading margin stability is maximized in coordination with total power losses. The following equation describes the combined objective function, in this study α is taken 0.5.

$$J_8(x,u) = \alpha \times J_3(x,u) + (1-\alpha) \times J_2(x,u), \quad 0 \le \alpha \le 1 \tag{27}$$

9. Maximization of loading margin stability and total voltage deviation

In this case, the loading margin stability is maximized in coordination with total voltage deviation. The following equation describes the combined objective function:

$$J_9(x,u) = \alpha \times J_3(x,u) + (1-\alpha) \times J_1(x,u), \quad 0 \le \alpha \le 1 \tag{28}$$

10. Critical reactive margin security

At critical situations such as load growth and contingency, it is important to maintain reactive power of generating units at security levels. Optimal coordination of reactive power delivered by generating units and multi-shunt FACTS devices is an important task to enhance the stability of power systems. In this study, two indices are proposed to measure and evaluate the performance of practical power systems.

$$\mathrm{CRMS}_i = \begin{cases} \mathrm{abs}\left(\dfrac{\mathrm{QG}_i}{\mathrm{QG}_{\min}}\right) & \text{if } \mathrm{QG}_i < 0 \\ \left(\dfrac{\mathrm{QG}_i}{\mathrm{QG}_{\max}}\right) & \text{if } \mathrm{QG}_i > 0, \quad i = 1, \ldots, \mathrm{NG} \end{cases} \tag{29}$$

11. Global reactive margin security

The higher GRMS indicates the higher degree of security and stability of power system. This index must be considered in coordination with other control variables to maintain the power system at reliable situation.

$$\mathrm{GRMS} = \frac{1}{\sum_{i=1}^{\mathrm{NG}} \mathrm{CRMS}_i} \tag{30}$$

3 Algorithm description

Very recently, a new interactive optimization algorithm was proposed for solving optimization problems. The particularity of the SCA can be outlined as follows:

1. The SCA creates multiple initial random candidate solutions and requires them to fluctuate outwards or toward the best solution [27] based on sine and cosine functions.

Fig. 2 Basic steps of the SCA

-Initialize a set of search agents (solution) (X)
Do
Evaluate each of the search agents by the objective function
Update the best solution found so far (P=X)
Update r1, r2, r3, and r4
Update the position of search agents using equation (31)
While (it < it max)
Return the best solution obtained so far as the global optimum

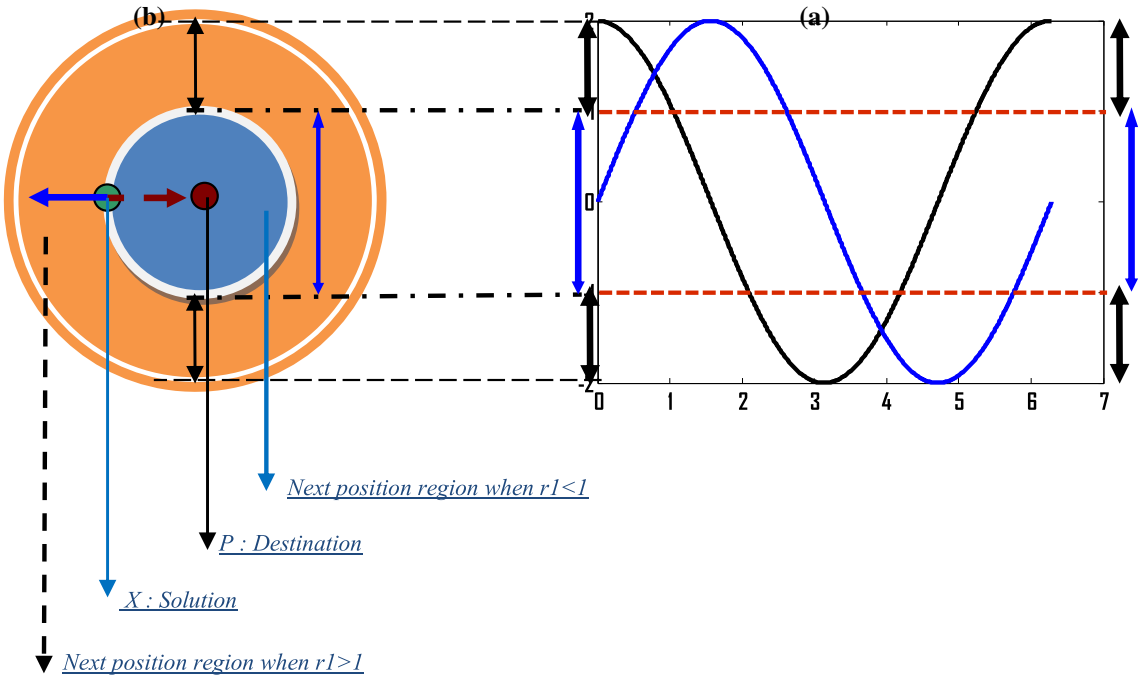

Fig. 3 Effects of sin and cosine on search process

2. Exploration phase is performed when the *sin* and *cosine* functions return a value greater than 1 or less than −1.
3. The exploitation phase is performed when *sin* and *cosine* functions return value between 1 and −1.
4. A specified random and adaptive variables are intergraded within the algorithm to balance between exploration and exploitation during search process. The basic steps of the SCA are presented in Fig. 2. The structure of the standard mechanism search of the SCA can be summarized as follows [27].

Phase 1: *Generate random solution* Like many population-based optimization techniques, the SCA starts the optimization search process with a random solution. Figure 3 shows the standard *sin cosine* search process transition.

Phase 2: *Evaluate and update solution* This random solution is evaluated repeatedly by a specified objective function and improved by a set of rules for exploration and exploitation stages. These two equations updated based on a switching parameter and are expressed as follows:

$$X_i^{it+1} = \begin{cases} X_i^{it} + r_1 \times \sin(r_2) \times \left| r_3 P_i^{it} - X_i^{it} \right|, & r_4 \prec 0.5 \\ X_i^{it} + r_1 \times \cos(r_2) \times \left| r_3 P_i^{it} - X_i^{it} \right|, & r_4 \geq 0.5 \end{cases} \tag{31}$$

where X_i^{it} is the position of the current solution in i-th dimension at it-th iteration, $r_1/r_2/r_3$ are random numbers, P_i^{it} is the destination point in i-th dimension.

r_1: is designed to guide the next position's region, which may be between the solution and destination or outside it. In order to achieve balance between exploration and exploitation phase, this parameter is dynamically adjusted during search process using the following equation:

$$r_1 = a - it \times \frac{a}{it\ \max} \tag{32}$$

where it is the current iteration, a is a constant and $it\ max$ is the maximum number of iteration

r_2: is designed to decide how far the movement should be toward or outward the destination.

r_3: is a random weighting parameter.

r_4: is a switching parameter that switches the transition between the sine and cosine components in Eq. (31).

The effects of sin and cosine on the search process are well illustrated in Fig. 3. For exploring the search space, the solutions should be able to search outside the space between their corresponding destinations as well. This can be achieved by changing the range of the sine and cosine functions as shown in Fig. 3a.

Figure 3b shows how changing the range of sine and cosine functions requires a solution to update its position outside or inside the space between itself and another solution [27]. Therefore, this search mechanism guarantees an efficient balance between exploration and exploitation.

4 Proposed power system planning strategy

The main contribution of the proposed planning strategy is its ability to locate the maximum loading margin stability under critical situations such as contingency. Firstly and in order to reduce the search space the SCA is performed in parallel to locate the suboptimal solutions at different levels of GRMS to generate initial database. Secondly, the basic SCA is modified by dynamically adjusting particular parameters during search process to well creating balance between *exploration* and *exploitation* phases.

Based on schematic representation shown in Fig. 4, the following points summarize the novelty and particularity of the proposed mechanism search introduced within the modified SCA.

1. Stage 1: *Generate initial database* In this stage, the two objective functions are optimized at different levels of GRMS. This first operation contributes to locate the suboptimal solutions, three GRMS have been considered.
2. Stage 2: At the first trial, the three suboptimal solutions found during the first stage are considered as an initial solution to the first SCA1. During this stage, two SCAs are executed, SCA1 receive the first initial population without considering different levels of GRMS, and SCA2 receive the subpopulations considering different levels of GRMS. Figure 4 shows the mechanism search of the proposed planning strategy.
3. Stage 3: The control variables associated with the new suboptimal solutions achieved during the first trial are saved and considered as an initial solution. In order to make diversity in search space, the worst solution found is considered within the best solution during the successes trials. The search process will stop until the maximum number of trial is reached.

4.1 Micro sine cosine procedure

The main task of this procedure is to achieve a refined local search space to enhance the final solution. The idea consists by dynamically adjusting the limits of control variables during search process. As well shown in Fig. 5, this routine allows the location of the best solution among many suboptimal solutions. The proposed procedure coordinated with the global search enhances the solution by performing smooth search around the near suboptimal solutions. The following points summarize the steps of the mechanism search of the proposed procedure:

- Collect all suboptimal solutions named feasible regions
- Rank the selected regions based on their fitness function
- Select the best suboptimal solution, and update the lower limits of specified control variables
- Select the worst region, and update the higher limits of specified control variables
- Compare results, save all updated new control variables
- Local search process stopped until a specified number of iteration is reached, in this study the number of iteration is fixed based on subregions chosen, Itreg = 4.

4.2 Parameters tuning

As well known, choosing feasible parameters is an important task to achieve the best solution during search process. Like many metaheuristic methods, Sin cosine algorithm requires setting specified parameters, in general, setting of these parameters depend on the nature and complexity of the problem to be solved. In this study, it is clearly found that an important constant coefficient 'a' and three control parameters known as $r1$, $r2$ and $r3$ must be dynamically adjusted during search process to balance between exploration and exploitation to escape from the local optimum. In this study, the number of search agents is taken 30, the maximum num-

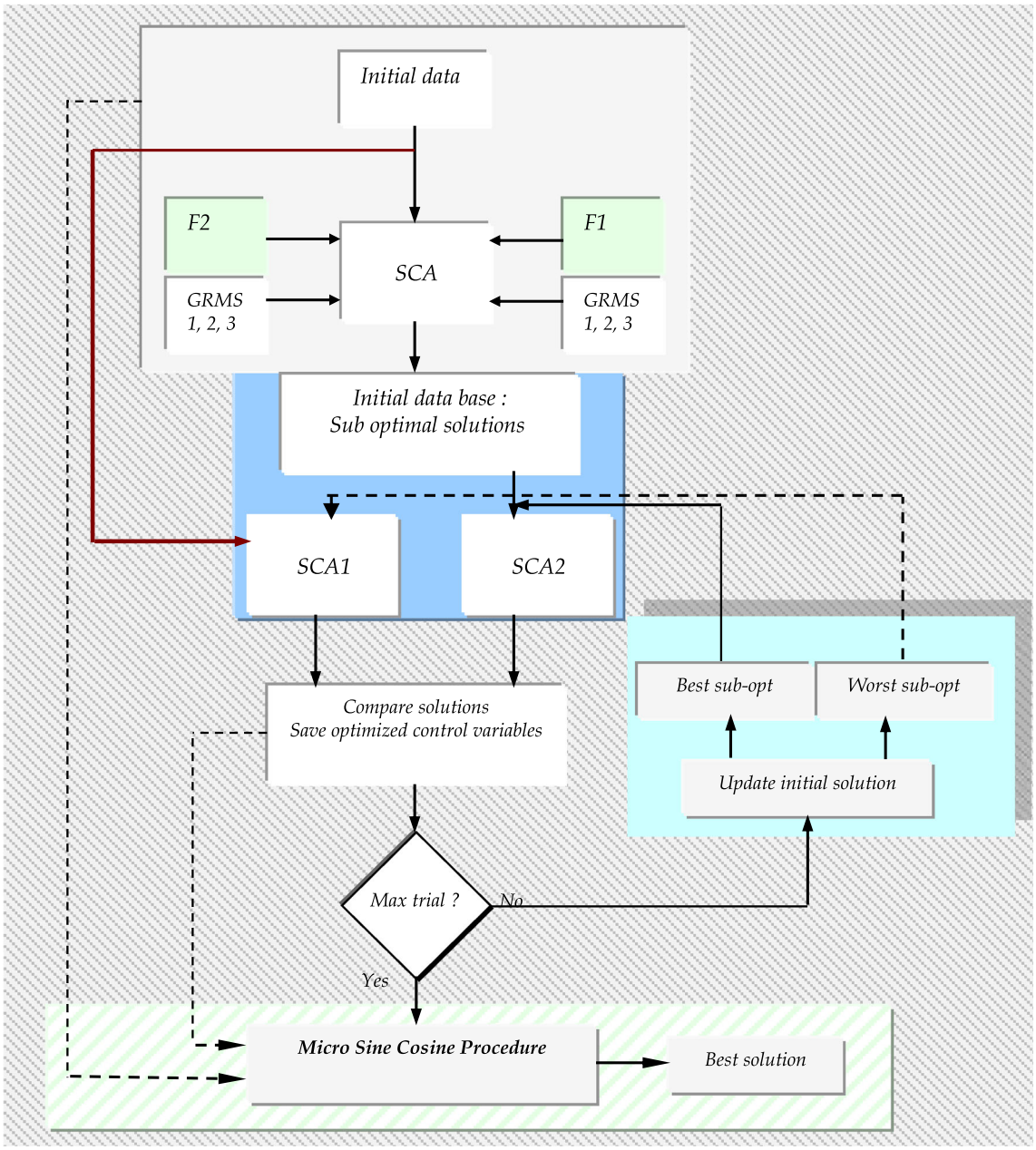

Fig. 4 Interactive mechanism search-based SCA

ber of iterations is taken between 80 and 200 based on the complexity of the problem to be solved, and the three parameters $r1$, $r2$, and $r3$ are taken as follows:

$$r_1 = a - it \times \frac{a}{it\,\max} \tag{33}$$

$$\text{with } a = 2 \times \left(1 - 0.5 \times \text{rand} \times \sin\left(\frac{it}{it\,\max}\right)\right) \tag{34}$$

$$r_2 = 2 \times \pi \times \text{rand} \tag{35}$$

$$r_3 = 2 \times \text{rand} \times \text{abs}\left(\sin\left(\frac{\text{rand}}{wf}\right)\right) \tag{36}$$

With, wf taken 100, the constant a is taken 2 only during the exploration stage at $it \leq itbase$.

5 Case studies and numerical results

Test System 1: IEEE 30 Bus

The first standard test system consists of 6 generating units located at buses: 1–2–5–8–11–13, four transformers located at lines 6–9, 6–10, 4–12 and 28–27 and nine shunt VAR compensation installed at buses 10, 12, 15, 17, 20, 21, 23, 24

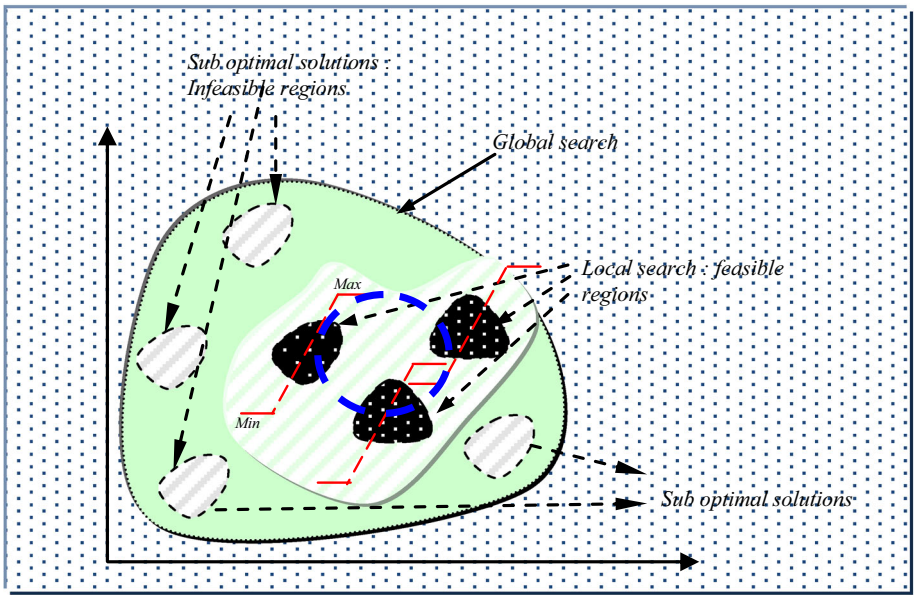

Fig. 5 Mechanism search of micro sine *cosine* procedure

and 29 [12, 17, 29]. To make flexible adjustment of reactive power exchanged between the compensators and the network, the nine shunt compensators are replaced with nine SVC devices. At normal condition, the total active and reactive load demand to satisfy are 283.4 MW and 126.2 MVAR, respectively. The technical data related to this test system are taken from [12,17], and the minimum and maximum limits of voltages at control buses and load buses are taken 0.9 and 1.1 p.u, respectively. The minimum and maximum limits of tap transformers are 0.9 and 1.1 p.u, respectively. Various combined objective functions have been considered such as: fuel cost, power loss, voltage deviation, voltage stability and loading margin stability.

Scenario 1 The main objective of this first scenario is to identify the capability of the practical power system in terms of reactive power management. Multi-suboptimal solutions are dynamically generated based on different levels of GRMS.

Case 1 Generation of global database based on GRMS for power loss minimization.

In this case, the total power loss has been optimized using SCA at different levels of GRMS. All optimized control variables are saved in an initial database as well shown in Table 1, all security constraints are within the margin security. Figure 6 shows the evolution GRMS and CRMS for four levels, as well depicted in Table 1, and the best total power loss achieved is **2.9913** MW; this value is obtained at low security level (GRMS = 0.6338 p.u); however, the total power loss **3.3582** MW has been achieved at high security level (GRMS = **1.3598** p.u). This initial database will be used in the next stage to optimize the loading margin stability under contingency.

Case 2 Generation of global database based on GRMS for voltage deviation minimization considering total power loss.

In this case, the total voltage deviation is also optimized using SCA. All suboptimal solutions found at different levels of GRMS are saved in an initial database. Figure 7 shows the evolution of GRMS and CRMS indices for four levels, as well depicted in Table 2, the best voltage deviation achieved is **0.2698** p.u, this value is obtained at high security level (GRMS = **0.9931** p.u). It is important to confirm that all security constraints are within their margin security. This initial database will be used in the next stage to optimize the loading margin stability under contingency.

Case 3 Generation of global database based on GRMS for voltage deviation minimization considering fuel cost.

In this case, the total voltage deviation is optimized in coordination with cost. All suboptimal solutions found at different levels of GRMS are saved in an initial database. Figure 8 shows the evolution GRMS and CRMS indices for four levels, as well depicted in Table 3, the best voltage deviation and total cost are **0.2453** p.u and **802.3510** $/h, respectively, this value obtained at high security level (GRMS = **0.9015** p.u).

Case 4 Generation of global database based on GRMS for power loss minimization considering fuel cost.

In this case, the total power loss is optimized in coordination with total fuel cost. All optimized control variables are saved in an initial database. The evolution of GRMS and CRMS indices at different levels is shown in Fig. 9. As well depicted in Table 4, the best total power loss and total cost achieved are **4.6819** MW, and **874. 23.37** $/h,

Table 1 Optimal setting of control variables: case 1: power loss optimization

Control variables		Level 1		Level 2		Level 3		Level 4	
P_{G1}	Q_{G1}	65.2911	−9.9058	65.3227	−4.9994	65.3817	7.8687	65.4482	22.3694
P_{G2}	Q_{G2}	66.1002	7.1626	66.1411	7.4967	66.2308	16.6667	66.3116	12.4497
P_{G5}	Q_{G5}	50.0000	21.9416	50.0000	19.9994	49.9997	13.3297	49.9994	9.9784
P_{G8}	Q_{G8}	35.0000	29.7646	35.0000	14.9998	34.9999	9.9971	34.9996	7.4832
P_{G11}	Q_{G11}	30.0000	7.7437	30.0000	12.4998	29.9999	8.3314	29.9997	6.2391
P_{G13}	Q_{G13}	40.0000	5.1420	40.0000	14.2638	39.9998	9.9978	39.9996	7.4903
V_{G1}		1.1000		1.1000		1.1000		1.1000	
V_{G2}		1.0956		1.0937		1.0900		1.0844	
V_{G5}		1.0784		1.0731		1.0582		1.0475	
V_{G8}		1.0858		1.0760		1.0609		1.0510	
V_{G11}		1.1000		1.0914		1.0740		1.0737	
V_{G13}		1.1000		1.1000		1.0849		1.0854	
T_{11}		1.0042		1.0242		1.0144		1.0000	
T_{12}		0.9950		1.0150		1.0052		0.9908	
T_{15}		0.9882		1.0082		0.9984		0.9840	
T_{36}		0.9812		1.0012		0.9914		0.9770	
$Qc10$		4.8881		4.8676		4.8239		4.9138	
$Qc12$		3.2196		3.2060		3.1772		3.2365	
$Qc15$		2.9329		2.9206		2.8944		2.9484	
$Qc17$		4.9276		4.9069		4.8628		4.9535	
$Qc20$		3.8217		3.8056		3.7715		3.8418	
$Qc21$		4.9376		4.9168		4.8727		4.9635	
$Qc23$		2.6958		2.6845		2.6604		2.7100	
$Qc24$		4.9376		4.9168		4.8727		4.9635	
$Qc29$		2.0441		2.0355		2.0172		2.0548	
Cost ($/h)		941.4216		941.6664		942.1742		942.6636	
Power loss (MW)		**2.9913**		**3.0638**		**3.2118**		**3.3582**	
Voltage deviation (p.u)		1.8970		1.5270		1.3019		1.3532	
GRMS (p.u)		0.6338		0.7618		1.1461		**1.3598**	
CRMS (p.u)		**0.4961**		0.2500		0.1667		0.1248	

The bold values indicate the best results found using the proposed algorithm

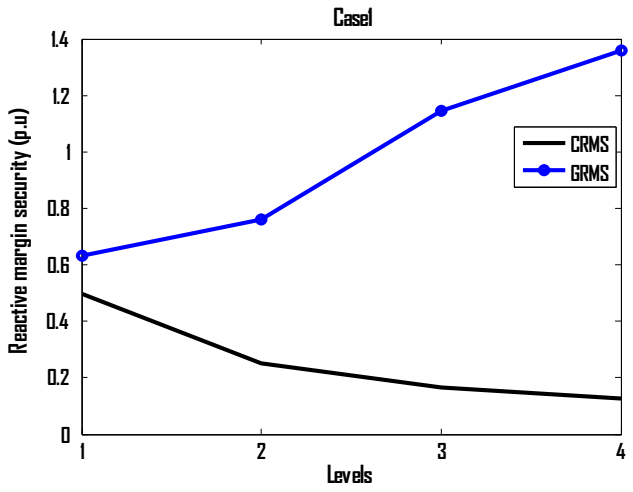

Fig. 6 Evolution of GRMS and CRMS: case 1

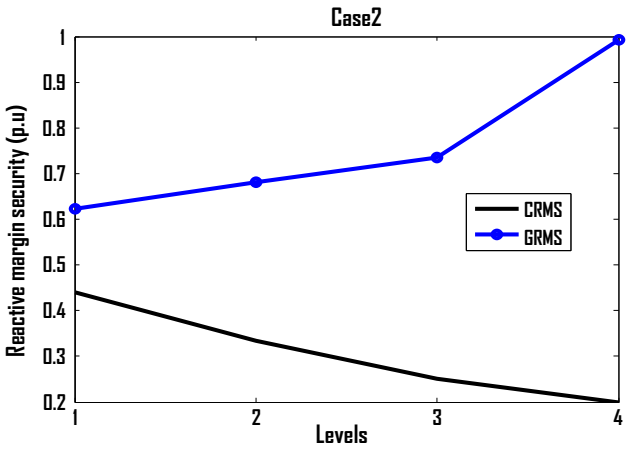

Fig. 7 Evolution of GRMS and CRMS: case 2

Table 2 Optimal setting of control variables: case 2: voltage deviation optimization

Control variables	Level 1	Level 2	Level 3	Level 4
Cost ($/h)	942.8374	942.8649	943.0858	943.1740
Power loss (MW)	3.4049	3.4137	3.4812	**3.5085**
Voltage deviation (p.u)	0.3035	0.2867	0.3141	**0.2698**
GRMS (p.u)	0.6219	0.6812	0.7350	**0.9931**
CRMS (p.u)	**0.4409**	0.3333	0.2500	0.2000

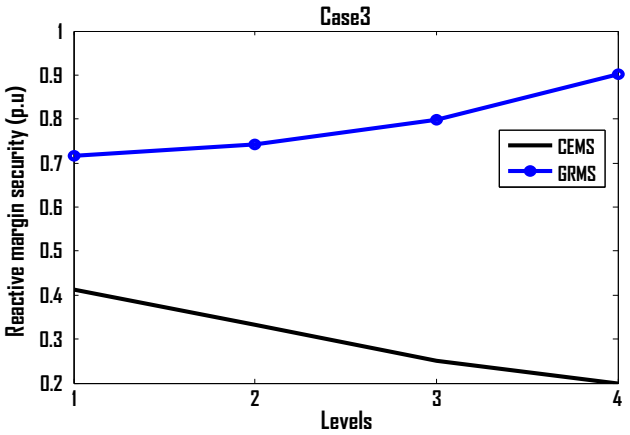

Fig. 8 Evolution of GRMS and CRMS: case 3

Table 3 Optimal setting of control variables: case 3: voltage deviation optimization considering fuel cost

Control variables	Level 1	Level 2	Level 3	Level 4
Cost ($/h)	**801.8693**	**801.9100**	**802.0120**	**802.3510**
Power loss (MW)	9.3810	9.3918	9.4161	9.5010
Voltage deviation (p.u)	**0.2917**	**0.3085**	**0.2507**	**0.2453**
GRMS (p.u)	0.7162	0.7431	0.7983	**0.9015**
CRMS (p.u)	**0.4121**	0.333	0.25	0.20

The bold values indicate the best results found using the proposed algorithm

respectively, and these values obtained at high security level (GRMS=**1.2265** p.u). This initial database will be used in the next stage to optimize the loading margin stability under contingency.

Scenario 2 The second scenario focused to demonstrate the superiority of the proposed security planning strategy-based interactive sine cosine algorithm to improve the solution of the standard OPF considering three objective functions such as total fuel cost, the total power loss and total voltage deviation, and these objective functions have been optimized individually and in coordination.

Case 5 Fuel cost minimization.

This first case of this second scenario focused on the minimization of the total fuel cost. The best total fuel cost

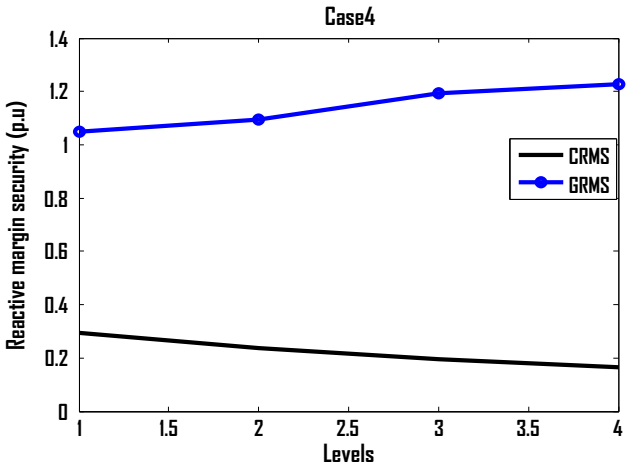

Fig. 9 Evolution of GRMS and CRMS: case 4

Table 4 Optimal setting of control variables: case 4: power loss optimization considering fuel cost

Control variables	Level 1	Level 2	Level 3	Level 4
Cost ($/h)	**865.4904**	**867.6137**	**869.7962**	**874.2337**
Power loss (MW)	**4.7885**	**4.7486**	**4.8190**	**4.6819**
Voltage deviation (p.u)	0.5042	0.4976	0.5244	0.4935
GRMS (p.u)	1.0474	1.0952	1.1946	**1.2265**
CRMS (p.u)	**0.2958**	0.2361	0.1935	0.1663

The bold values indicate the best results found using the proposed algorithm

optimized is **798.9513** $/h, and the corresponding power loss, voltage deviation and voltage stability index are 8.5950 MW, 1.9473 p.u, and 0.1264 p.u, respectively. Detailed results for optimal setting of control variables are shown in Table 5.

Case 6 Power loss minimization.

This case focused on the demonstration of the proposed planning strategy on the optimization of total power loss. The best total active power loss achieved is **2.8434** MW, which is better than the results of many papers cited in the literature [12,17]. The convergence characteristic for total power loss minimization is shown in Fig. 10. Detailed results of optimal setting of control variables are depicted in Table 5, and all security constraints are within their admissible limits.

Case 7 Voltage deviation minimization.

This case focused on the minimization of the total voltage deviation. The best total voltage deviation achieved is **0.1172** p.u, which is better than the results found in many recent papers, cited in the literature, and the convergence characteristic for voltage deviation minimization is shown in Fig. 11. Detailed results of optimal setting of control variables are depicted in Table 5. All security constraints are within their admissible limits

Table 5 Optimal setting of control variables cases: 5–6–7–8–9–10

Control variables	Case 5	Case 6	Case 7	Case 8	Case 9	Case 10
P_{G1} (Slack)	177.1105	51.8115	129.8550	176.6697	100.3971	54.5004
P_{G2}	48.6898	79.5977	53.4565	48.7329	59.7567	78.7221
P_{G5}	21.3040	49.9343	44.6192	21.5413	44.4991	49.3850
P_{G8}	21.0310	34.9643	29.7379	21.8424	31.7139	34.5797
P_{G11}	11.8592	29.9717	20.2644	12.1127	23.4825	29.6420
P_{G13}	12.0007	39.9639	12.0002	12.0013	28.2331	39.5243
V_{G1}	1.1000	1.1000	1.0129	1.0717	1.0901	1.1000
V_{G2}	1.0876	1.0971	1.0042	1.0448	1.0703	1.0972
V_{G5}	1.0612	1.0791	1.0139	0.9987	1.0313	1.0792
V_{G8}	1.0690	1.0859	1.0024	1.0038	1.0353	1.0860
V_{G11}	1.1000	1.0996	1.0519	1.0328	1.0332	1.0997
V_{G13}	1.1000	1.0999	1.0141	1.0439	1.0448	1.1000
T_{11}	1.0366	1.0422	1.0693	1.0090	1.0267	1.0042
T_{12}	0.9005	0.9123	0.9005	0.9998	1.0174	0.9164
T_{15}	0.9739	0.9795	0.9769	0.9930	1.0106	0.9415
T_{36}	0.9633	0.9689	0.9709	0.9860	1.0036	0.9309
$Qc10$	3.4519	4.8651	3.4528	3.4492	3.4822	4.8225
$Qc12$	4.8335	3.2044	4.8347	4.8296	4.8758	3.1763
$Qc15$	2.5407	2.9191	2.5413	2.5386	2.5629	2.8935
$Qc17$	4.8345	4.9044	4.8357	4.8306	4.8768	4.8614
$Qc20$	4.2549	3.8037	4.2560	4.2515	4.2922	3.7704
$Qc21$	4.8275	4.9143	4.8287	4.8237	4.8698	4.8712
$Qc23$	4.8093	2.6832	4.8105	4.8055	4.8514	2.6597
$Qc24$	4.8345	4.9143	4.8357	4.8306	4.8768	4.8712
$Qc29$	2.7322	2.0345	2.7329	2.7300	2.7561	2.0167
Cost ($/h)	**798.9517**	965.6577	850.2329	**802.3490**	**874.2353**	**959.0448**
Power loss (MW)	8.5952	**2.8434**	6.5332	9.5003	**4.6824**	**2.9536**
Voltage deviation (p.u)	1.9474	2.0678	**0.1172**	**0.2455**	0.4938	**2.4338**
Voltage stability Lmax (p.u)	0.1264	0.1253	0.1493	0.1493	0.1456	**0.1192**

The bold values indicate the best results found using the proposed algorithm

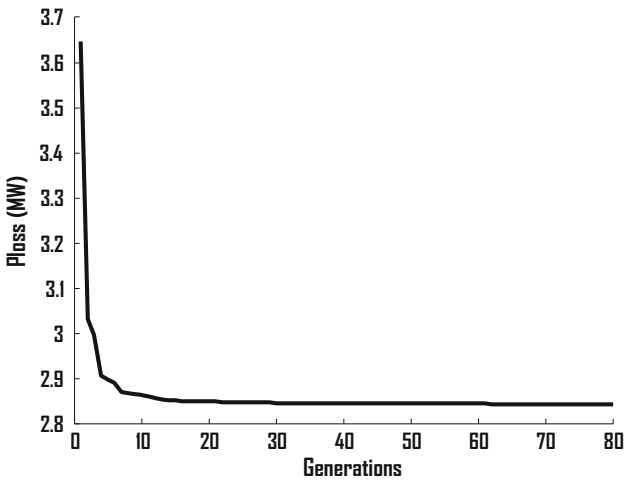

Fig. 10 Convergence characteristic: last stage, case 6

Case 8 Voltage deviation and cost minimization.

In practical situations, it is useful to find the best compromise solutions between two objective functions. This case is investigated to optimize the total voltage deviation considering fuel cost. The best total voltage deviation achieved is **0.2455** p.u, which is higher than case 7; however, the total cost obtained is reduced to a lower value 802.3490 $/h. For this case, the voltage stability index achieved is 0.1493 p.u. All control variables and state variables such as reactive power of generating units, voltage magnitudes at load buses, and power transit in branches are within their security limits.

Case 9 Power loss and cost minimization.

In order to show the relation between power loss and total fuel cost, the total power loss is optimized considering the

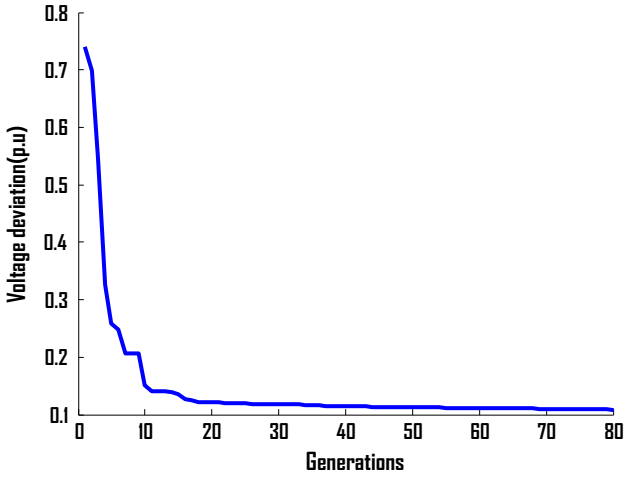

Fig. 11 Convergence characteristic: last stage, case 7

generation cost. For this case, the total power loss optimized is **4.6824** MW, the optimized active power loss for this case is increased compared to case 6; however, the corresponding total fuel cost achieved is reduced to 874.2353. It is important to confirm that the optimal solution is achieved without violation of all control and state variables.

Case 10 Voltage stability index minimization considering total active power loss at normal condition.

Voltage stability is an important index which reflects the reliability of practical power system to deliver energy quality to consumer under disturbances such as load growth and faults at particular important branches. Therefore, the minimization of voltage stability index is a significant objective function. In this case, and by using the proposed algorithm, the voltage stability index is optimized in coordination with power loss. The voltage stability index is considerably decreased in this case to **0.1192** p.u compared to all cases (5–9). It is important to confirm that the optimized *L_index* value is achieved at lower total power loss (**2.9536** MW), and the corresponding total fuel cost and total voltage deviation are 959.0448 $/h and 2.4338 p.u, respectively. It can be seen clearly that the voltage stability index is improved compared to all previous cases; thus, the distance from breakdown point is improved. The optimal control variables related to this case are depicted in Table 5, and it can be seen that all the control variables are within their upper and lower limits.

5.1 Comparative study

In order to evaluate the particularity and performances of the proposed planning strategy considering critical situations, it has been compared with various recent optimization algorithms. Table 6 shows a comparative study in terms of solution quality with several recent optimization methods. It is evident that the quality of results achieved using the proposed power system planning strategy-based modified *sine cosine* algorithm is better compared with many recently published OPF.

Scenario 3 Security OPF considering loading margin stability with and without contingency

Case 11 Maximization of loading margin stability considering total loss without contingency.

The main objective function named loading margin stability is optimized considering the total power loss. The optimized loading margin stability achieved in coordination with power loss is **1.48796** p.u and **13.3120** MW, respectively, and the corresponding total voltage deviation and voltage stability index are **1.4773** p.u and 0.2002 p.u, respectively. Table 7 shows the setting control variables found associated with the best loading margin stability achieved in coordination with total power loss. Figure 12 shows the repartition of voltage magnitudes at all buses. All security constraints such as reactive power of generation units, voltage magnitudes, and power transit in branches are within their security limits.

Case 12 Maximization of loading margin stability considering voltage deviation without contingency.

In this case, the loading margin stability is optimized considering the total voltage deviation. The optimized loading margin stability achieved in coordination with voltage deviation is **1.480 p.u, 0.2771 p.u**, respectively, and the corresponding total power loss and voltage stability index are **14.3232** MW and 0.2217 p.u, respectively; as we can see in Table 7, the total voltage deviation is improved compared to case 8. Table 7 shows the setting control variables found associated with the best loading margin stability achieved in coordination with total voltage deviation. The distribution of voltage magnitudes at all buses is shown in Fig. 12. Also for this critical case, all security constraints such as reactive power of generation units, voltage magnitudes, and power transit in branches are within their admissible limits.

Case 13 Maximization of loading margin stability considering total voltage deviation under contingency.

This case is investigated to validate the extensibility and efficiency of the proposed security planning strategy by maximization the loading margin stability considering total voltage deviation at critical situations such as contingency at specified branches. By considering contingency at branch **2–5**, the total loading margin stability maximized to **1.24** p.u, and the corresponding total voltage deviation and total power loss achieved are **0.2505** p.u and **16.0968** MW, respectively. The distribution of voltage magnitudes at all buses is shown in Fig. 12. It is important to confirm that all security constraints are satisfied.

Table 6 Comparative study: best solutions: casees 5–6–7

Methods: Refs. [12,17]	Optimal results			
	Cost ($/h)	Power loss (MW)	Voltage deviation (p.u)	Voltage stability (p.u)
TLBO	799.0715	–	–	
GSA	798.6751*	–	–	
DSA	799.0943	–	–	
BBO	799.1116	–	–	
DE	799.2891	–	–	
SA	799.4500	–	–	
AGAPOP	799.8441	–	–	
BHBO	799.9217	–	–	
EM	800.0780	–	–	
EADHDE	800.1579	–	–	
EADDE	800.2041	–	–	
PSO	800.4100	–	–	
FPSO	800.7200	–	–	
IGA	800.8050	–	–	
PSO	800.9600	–	–	
GAF	801.2100	–	–	
ICA	801.8430	–	–	
EGA	802.0600	–	–	
TS	802.2900	–	–	
MDE	802.3760	–	–	
IEP	802.4650	–	–	
EP	802.6200	–	–	
RGA	804.0200	–	–	
GM	804.8530	–	–	
GA	805.9400	–	–	
GWO	–	2.9377	–	
ABC	–	3.0410	–	
MOEA/D [17]	799.5300	2.8812	0.0998	
GSO [18]	799.0600	–	–	
DSA [19]	800.3887	3.09450	–	
FHSA [15]	799.9140	–	–	
ARCBBO [23]	800.5159	3.1009	0.0920	
MSA [20]	800.5099	3.1005	0.10842	0.13713
Proposed approach ISCA	**798.9517**	**2.8434**	**0.1172**	**0.1192**

The bold values indicate the best results found using the proposed algorithm

Case 14 Maximization of loading margin stability and minimization of total power loss under contingency.

This case is dedicated to show the impact of contingency on the optimized value of loading margin stability considering the total power loss of the system. By considering contingency at branch 2–5, the total loading margin stability maximized at **1.25** p.u, the corresponding total power loss and voltage deviation achieved are **14.9784** MW and **1.6720** p.u, respectively. The distribution of voltage magnitudes at all buses is shown in Fig. 12. It is important to confirm that all security constraints such as voltage magnitudes at all load buses, reactive power of generating units and power transit in branches are within their security limits. Figure 13 shows that the power transit magnitudes in all branches are within their security limits. for cases 11, 12, 13, 14.

Case 15 Maximization of loading margin stability and minimization of voltage stability under contingency.

This case focused to demonstrate the efficiency and particularity of the proposed planning strategy in solving security OPF under various practical and critical situations. For this case, the loading margin stability is optimized in coordination with voltage stability under severe contingency such as

Table 7 Optimal setting of control variables: cases: 11–12–13–14

Control variables	Min	Max	Case 11	Case 12	Case 13	Case 14	Case 15
P_{G1} (Slack)	50	200	200.0000	198.7552	186.7722	187.1725	187.1949
P_{G2}	20	80	80.0000	80.0000	25.7404	27.0559	27.0850
P_{G5}	15	50	50.0000	50.0000	50.0000	50.0000	50.0000
P_{G8}	10	35	35.0000	35.0000	34.9999	35.0000	35.0000
P_{G11}	10	30	30.0000	30.0000	29.9999	30.0000	30.0000
P_{G13}	12	40	40.0000	40.0000	39.9999	40.0000	40.0000
V_{G1}	0.95	1.1	1.1000	1.0750	1.0718	1.1000	1.1000
V_{G2}	0.95	1.1	1.0885	1.0516	1.0524	1.0829	1.0813
V_{G5}	0.95	1.1	1.0567	1.0082	0.9632	0.9896	0.9871
V_{G8}	0.95	1.1	1.0659	1.0097	1.0192	1.0600	1.0580
V_{G11}	0.95	1.1	1.1000	1.0498	1.0593	1.1000	1.1000
V_{G13}	0.95	1.1	1.1000	1.0306	0.9818	1.1000	1.1000
T_{11}	0.90	1.1	1.0275	1.0150	1.0250	1.0184	1.0102
T_{12}	0.90	1.1	0.9125	0.9000	0.9100	0.9034	0.9162
T_{15}	0.90	1.1	0.9794	0.9670	0.9770	0.9703	0.9621
T_{36}	0.90	1.1	0.9574	0.9450	0.9550	0.9483	0.9401
$Qc10$	0	5	5.0000	5.0000	5.0000	5.0000	5.0000
$Qc12$	0	5	5.0000	5.0000	5.0000	5.0000	5.0000
$Qc15$	0	5	5.0000	5.0000	5.0000	5.0000	5.0000
$Qc17$	0	5	5.0000	5.0000	5.0000	5.0000	5.0000
$Qc20$	0	5	5.0000	5.0000	5.0000	5.0000	5.0000
$Qc21$	0	5	5.0000	5.0000	5.0000	5.0000	5.0000
$Qc23$	0	5	5.0000	5.0000	5.0000	5.0000	5.0000
$Qc24$	0	5	5.0000	5.0000	5.0000	5.0000	5.0000
$Qc29$	0	5	5.0000	5.0000	5.0000	5.0000	5.0000
Loading margin stability λ (p.u)	–	–	**1.48796**	**1.480**	**1.24**	**1.25**	**1.25**
Fuel cost ($/h)			1404.70	1400.40	1163.7	1168.6	1168.8
Power loss (MW)	–	–	**13.3120**	14.3232	16.0963	**14.9784**	15.0299
Voltage deviation (p.u)	–	–	1.4773	**0.2771**	**0.2505**	1.6701	1.6948
L_index (p.u)			**0.2002**	**0.2217**	**0.1831**	**0.1628**	**0.1616**
Base load (MW)			283.4	283.4	283.4	283.4	283.4
New load (MW)			**421.6879**	**419.4320**	**351.4160**	**354.250**	**354.250**
Total system capacity (MW)			435.00	435.00	435.500	435.00	435.00
Contingency in branches			Without	Without	**2–5**	**2–5**	**2–5**

The bold values indicate the best results found using the proposed algorithm

fault at the important branch (2–5). In such critical situation, it is important to maintain the voltage stability index at all load buses far from the breakdown point. Compared to all cases and in particular to case 13, the voltage stability index is improved to **0.1616** p.u at loading margin stability **1.25** p.u. However, the voltage deviation is increased to 1.6948 p.u compared to the optimized value 0.2505 p.u found at loading margin stability 1.24 p.u.

Test System 2: IEEE 118-Bus

The robustness of the proposed strategy is validated on a large practical electrical test system IEEE 118-bus. The network consists of 186 branches, 54 generator buses and 14 capacitor banks, and nine branches 8–5, 26–25, 30–17, 38–37, 63–59, 64–61, 65–66, 68–69, and 81–80 are tap changing transformers [12,17,28]. The total load demand to satisfy is 4242 MW for active power and 8777 MVAR for reactive power, the limits values of voltages for all generating units and tap setting transformer control variables are considered to be 1.1–0.9 in p.u, and the maximum and minimum values for voltages at all load buses are 1.1 and 0.9 in p.u, respectively. For this second test system, three objective functions are considered:

Case 16: Minimization of voltage deviation with and without SVC devices at normal condition

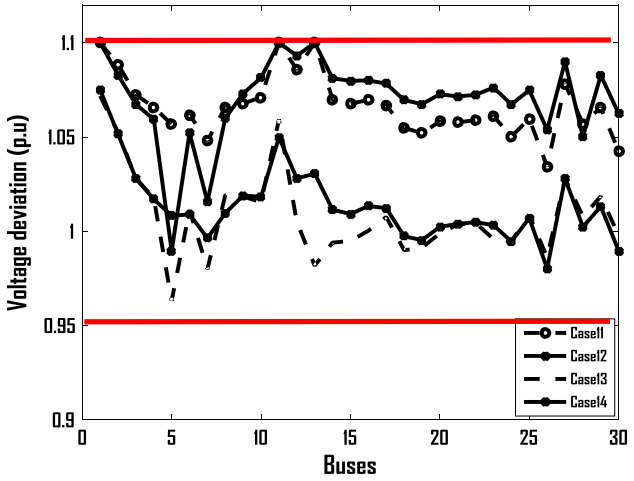

Fig. 12 Voltage profiles: cases: 11–12–13–14

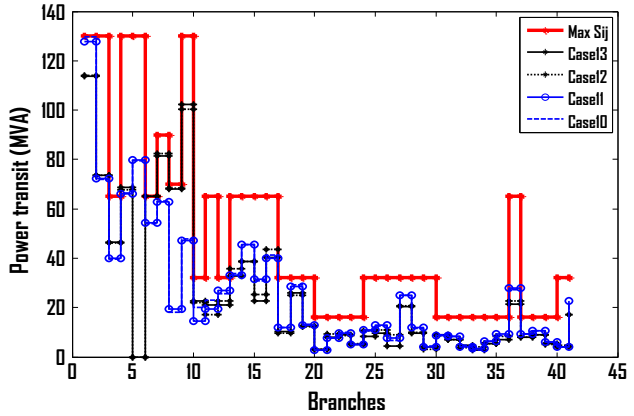

Fig. 13 Power transit magnitudes (MVA): cases: 11–12–13–14

Case 17: Maximization of loading margin stability considering total power loss
Case 18: Maximization of loading margin stability considering total voltage deviation

Case 16 Minimization of voltage deviation with and without SVC devices at normal condition.

In this case, the voltage deviation is minimized at normal condition with and without the effect of SVC devices. The best voltage deviation found without considering the SVC devices is **0.4540** p.u, the corresponding power loss achieved is 10.5694 MW, and by considering installation of multi-SVC devices installed at specified locations, the value of voltage deviation improved to **0.4072** p.u, and the corresponding power loss is 10.0370 MW. Convergence characteristics for voltage deviation achieved at the final stage using the *micro Sin Cosine* procedure are shown in Figs. 14 and 15. It is seen from Figs. 14 and 15, that the near optimal solution is located within 10–20 iterations, thus justifying the choice of

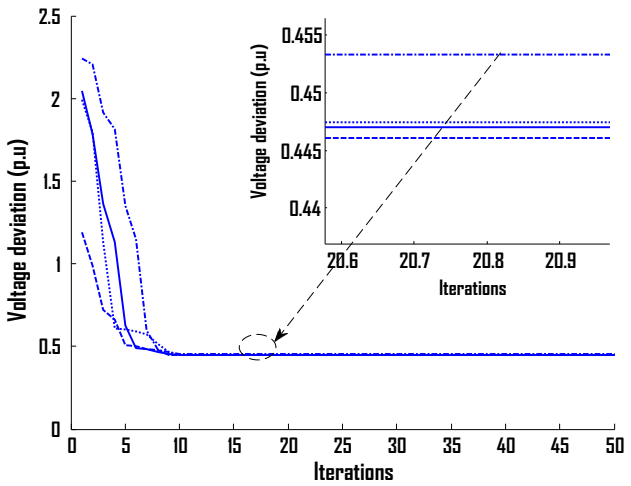

Fig. 14 Convergence characteristics (4 trials) for voltage deviation minimization without SVC devices: last stage: IEEE 118-Bus test system

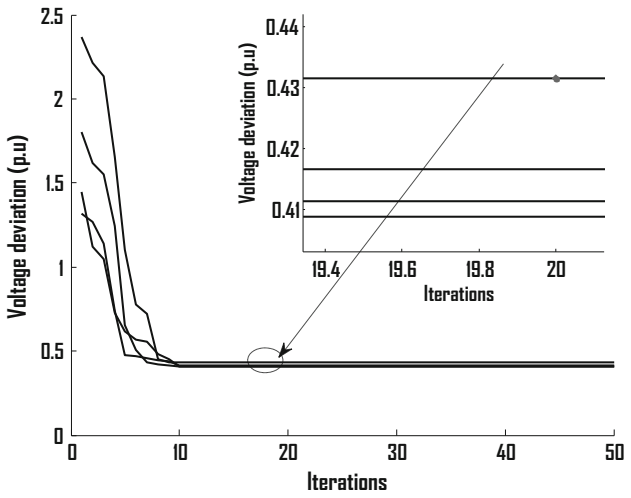

Fig. 15 Convergence characteristics (4 trials) for voltage deviation minimization with SVC devices: last stage: IEEE 118-Bus test system

the maximum number of iteration of 50. Due to the interactivity aspect of the proposed local search procedure, only four trials are sufficient to locate the best solution among the suboptimal solutions. It is also important to confirm that all constraints variables such as reactive power of generating units, and power transit in branches are within their security limits.

Case 17 Maximization of loading margin stability considering total power loss.

In this case, the vector control considered consists of active power and voltage control for generating units, tap transformer, and reactive power of SVC devices. For this case, the loading margin stability is maximized considering total power loss. The total loading margin stability achieved is **1.585** p.u (6723.6 MW), and the corresponding total power

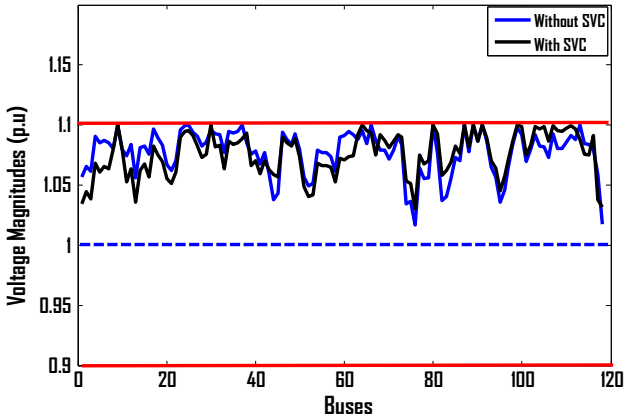

Fig. 16 Distribution of voltage magnitudes: case 17

loss and voltage deviation of the system are **46.8752** MW and **4.5311** p.u, respectively, without considering the SVC devices; however, by considering the integration of muti SVC devices at specified locations, the total power loss and voltage deviation are reduced to **43.9585** MW and **4.4239** p.u, respectively. All security constraints such as voltages at all buses, reactive power of generating units and power transit in branches are within their security limits. The distribution of voltage magnitudes at all buses is shown in Fig. 16. For this case, the optimized control variables with and without integration of SVC devices are depicted in Table 8.

Case 18 Maximization of loading margin stability considering total voltage deviation

Table 8 Optimized control variables for IEEE 118-bus system for case 17

Control variables	Without SVC	With SVC	Control variables	Without SVC	With SVC	Control variables	Without SVC	With SVC
P_{G1}	99.9999	99.9999	V_{G25}	1.1000	1.0957	$Qc105$	0	27.5208
P_{G4}	99.9998	99.9999	V_{G26}	1.0943	1.0911	$Qc107$	0	8.2562
P_{G6}	99.9999	99.9999	V_{G27}	1.0906	1.0822	$Qc110$	0	8.2562
P_{G8}	99.9998	99.9999	V_{G31}	1.0924	1.0821			
P_{G10}	130.3122	127.1409	V_{G32}	1.0923	1.0835			
P_{G12}	184.9999	184.9999	V_{G34}	1.0949	1.0864			
P_{G15}	99.9999	99.9999	V_{G36}	1.0946	1.0850			
P_{G18}	99.9999	99.9999	V_{G40}	1.0784	1.0703			
P_{G19}	99.9999	99.9999	V_{G42}	1.0774	1.0705			
P_{G24}	64.7077	63.4312	V_{G46}	1.0943	1.0899			
P_{G25}	0.0016	0.0015	V_{G49}	1.0927	1.0888			
P_{G26}	160.2803	159.3645	V_{G54}	1.0789	1.0683			
P_{G27}	99.9999	99.9999	V_{G55}	1.0774	1.0661			
P_{G31}	106.9999	106.9999	V_{G56}	1.0770	1.0660			
P_{G32}	99.9999	99.9999	V_{G59}	1.0898	1.0726			
P_{G34}	99.9999	99.9999	V_{G61}	1.0948	1.0735			
P_{G36}	99.9999	99.9999	V_{G62}	1.0922	1.0744			
P_{G40}	100.0000	100.0000	V_{G65}	1.0845	1.0954			
P_{G42}	100.0000	100.0000	V_{G66}	1.1000	1.0932			
P_{G46}	118.9999	118.9999	V_{G69}	1.0793	1.0873			
P_{G49}	303.9999	303.9999	V_{G70}	1.0716	1.0812			
P_{G54}	148.0000	148.0000	V_{G72}	1.0907	1.0921			
P_{G55}	100.0000	100.0000	V_{G73}	1.0836	1.0902			
P_{G56}	100.0000	100.0000	V_{G74}	1.0344	1.0536			
P_{G59}	254.9999	254.9999	V_{G76}	1.0166	1.0302			
P_{G61}	259.9998	259.9997	V_{G77}	1.0639	1.0749			
P_{G62}	99.9998	99.9998	V_{G80}	1.1000	1.1000			
P_{G65}	490.9995	490.9994	V_{G85}	1.0730	1.0825			
P_{G66}	223.3688	186.5071	V_{G87}	1.1000	1.1000			
P_{G69}	97.1415	109.0510	V_{G89}	1.1000	1.1000			
P_{G70}	99.9997	99.9998	V_{G90}	1.0868	1.0868			
P_{G72}	23.4978	24.0790	V_{G91}	1.1000	1.1000			

Table 8 continued

Control variables	Without SVC	With SVC	Control variables	Without SVC	With SVC	Control variables	Without SVC	With SVC
P_{G73}	32.3520	35.4804	V_{G92}	1.0867	1.0894			
P_{G74}	99.9999	99.9999	V_{G99}	1.0982	1.1000			
P_{G76}	99.9999	99.9999	V_{G100}	1.0920	1.0986			
P_{G77}	57.9673	99.9998	V_{G103}	1.0922	1.0989			
P_{G80}	576.9999	576.9999	V_{G104}	1.0823	1.0965			
P_{G85}	99.9998	99.9998	V_{G105}	1.0816	1.0989			
P_{G87}	26.6515	26.7863	V_{G107}	1.0930	1.0991			
P_{G89}	254.8056	242.8482	V_{G110}	1.0856	1.0972			
P_{G90}	99.9999	99.9999	V_{G111}	1.0915	1.0992			
P_{G91}	94.1983	91.6212	V_{G112}	1.0882	1.0969			
P_{G92}	99.9998	99.9998	V_{G113}	1.1000	1.0878			
P_{G99}	98.5610	82.6789	V_{G116}	1.0801	1.0910			
P_{G100}	191.6792	204.4337	$T1$	1.0120	1.0314	Tap transformers: p.u		
P_{G103}	36.7618	36.7146	$T2$	0.9863	1.0053			
P_{G104}	61.7019	61.7507	$T3$	0.9863	1.0053			
P_{G105}	99.8900	99.9508	$T4$	0.9606	0.9791			
P_{G107}	92.1433	91.9006	$T5$	0.9863	1.0053			
P_{G110}	78.0852	78.0246	$T6$	1.0120	1.0314			
P_{G111}	0.4094	0.3408	$T7$	0.9606	0.9791			
P_{G112}	99.9994	99.9994	$T8$	0.9606	0.9791			
P_{G113}	99.9335	99.4269	$T9$	0.9606	0.9791			
P_{G116}	99.9998	99.9998	$Qc5$	0	−55.0416	Reactive power of shunt SVC exchanged with the network (MVAR)		
V_{G1}	1.0570	1.0343	$Qc34$	0	19.2646			
V_{G4}	1.0903	1.0684	$Qc37$	0	−34.4010			
V_{G6}	1.0873	1.0656	$Qc44$	0	13.7604			
V_{G8}	1.0802	1.0801	$Qc45$	0	13.7604			
V_{G10}	1.0799	1.0799	$Qc46$	0	13.7604			
V_{G12}	1.0838	1.0634	$Qc48$	0	6.8802			
V_{G15}	1.0826	1.0676	$Qc74$	0	16.5125			
V_{G18}	1.0895	1.0753	$Qc79$	0	27.5208			
V_{G19}	1.0834	1.0695	$Qc82$	0	27.5208			
V_{G24}	1.0992	1.0946	$Qc83$	0	13.7604			
Ploss (MW)				**46.8752**	**43.9585**			
VD (p.u)				4.5311	4.4239			
LF (p.u)				**1.585**	**1.585**			

The bold values indicate the best results found using the proposed algorithm

In this case, the vector control considered contains active power and voltage control for generating units, tap transformer, and reactive power of SVC devices. For this case, the loading margin stability is maximized considering the total power loss. The total loading margin stability is achieved without considering the integration of SVC devices is **1.485** p.u, and the corresponding total voltage deviation and total power loss of the system are reduced to **1.5116** p.u and **38.4761** MW. By considering the integration of SVC devices at specified locations, and for the same loading margin stability, the voltage deviation improved to **1.0520** p.u, and the corresponding total power loss is **37.2839** MW. The distribution of voltage magnitudes at all buses is shown in Fig. 17. All security constraints such as voltages at all buses, reactive power of generating units and power transit in branches are within their security limits. For this case, the optimal control variables achieved with and without integration of SVC devices are depicted in Table 9.

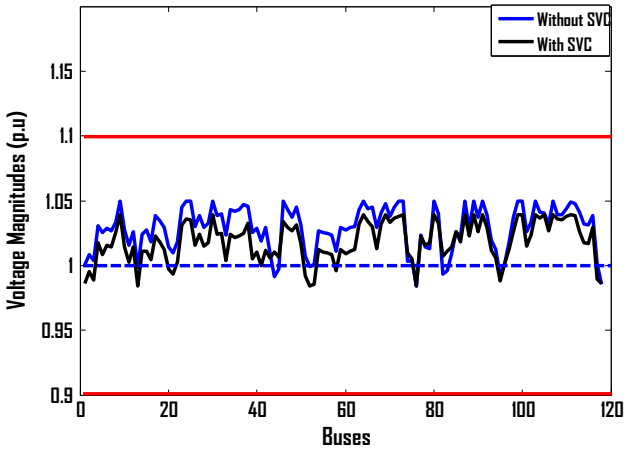

Fig. 17 Distribution of voltage magnitudes: case 18

6 Conclusion

In this paper, a novel optimization algorithm named interactive sine cosine algorithm is efficiently adapted and applied for solving the loading margin stability under contingency of practical power system. Firstly, in order to reduce the search space, the SCA is performed in parallel to locate the suboptimal solutions based on an initial database generated considering GRMS and CRMS indices. Secondly, the basic SCA is modified by dynamically adjusting particular parameters during search process to well creating balance between exploration and exploitation phases. The robustness of the proposed planning strategy in solving practical OPF problems is validated on a small and large test systems, the IEEE 30-Bus, and the IEEE 118-Bus considering load growth and

Table 9 Optimized control variables for IEEE 118-bus system for case 18

Control variables	Without SVC	With SVC	Control variables	Without SVC	With SVC	Control variables	Without SVC	With SVC
P_{G1}	100.0000	100.0000	V_{G25}	1.0495	1.0355	*Qc105*	0	39.4476
P_{G4}	99.9999	100.0000	V_{G26}	1.0303	1.0157	*Qc107*	0	11.8343
P_{G6}	100.0000	100.0000	V_{G27}	1.0384	1.0239	*Qc110*	0	11.8343
P_{G8}	99.9999	100.0000	V_{G31}	1.0388	1.0241			
P_{G10}	84.0977	86.0540	V_{G32}	1.0396	1.0251			
P_{G12}	185.0000	185.0000	V_{G34}	1.0432	1.0241			
P_{G15}	100.0000	100.0000	V_{G36}	1.0431	1.0230			
P_{G18}	100.0000	100.0000	V_{G40}	1.0290	1.0103			
P_{G19}	100.0000	100.0000	V_{G42}	1.0291	1.0118			
P_{G24}	54.2717	54.0481	V_{G46}	1.0495	1.0340			
P_{G25}	0.00050	0.00030	V_{G49}	1.0451	1.0311			
P_{G26}	117.2570	119.1585	V_{G54}	1.0270	1.0122			
P_{G27}	100.0000	100.0000	V_{G55}	1.0252	1.0101			
P_{G31}	107.0000	107.0000	V_{G56}	1.0249	1.0099			
P_{G32}	100.0000	100.0000	V_{G59}	1.0292	1.0123			
P_{G34}	100.0000	100.0000	V_{G61}	1.0296	1.0112			
P_{G36}	100.0000	100.0000	V_{G62}	1.0303	1.0125			
P_{G40}	100.0000	100.0000	V_{G65}	1.0436	1.0339			
P_{G42}	100.0000	100.0000	V_{G66}	1.0454	1.0302			
P_{G46}	119.0000	119.0000	V_{G69}	1.0478	1.0390			
P_{G49}	304.0000	304.0000	V_{G70}	1.0381	1.0330			
P_{G54}	148.0000	148.0000	V_{G72}	1.0500	1.0382			
P_{G55}	100.0000	100.0000	V_{G73}	1.0500	1.0390			
P_{G56}	100.0000	100.0000	V_{G74}	1.0029	1.0100			
P_{G59}	255.0000	255.0000	V_{G76}	0.9840	0.9843			
P_{G61}	259.6539	259.9998	V_{G77}	1.0236	1.0224			
P_{G62}	99.9999	100.0000	V_{G80}	1.0500	1.0390			
P_{G65}	487.7456	389.7723	V_{G85}	1.0259	1.0264			
P_{G66}	58.2861	98.0122	V_{G87}	1.0500	1.0390			
P_{G69}	42.9707	131.2486	V_{G89}	1.0500	1.0390			
P_{G70}	99.9999	100.0000	V_{G90}	1.0375	1.0264			

Table 9 continued

Control variables	Without SVC	With SVC	Control variables	Without SVC	With SVC	Control variables	Without SVC	With SVC
P_{G72}	21.5441	22.6905	V_{G91}	1.0500	1.0390			
P_{G73}	28.0776	33.4311	V_{G92}	1.0394	1.0294			
P_{G74}	100.0000	100.0000	V_{G99}	1.0500	1.0389			
P_{G76}	100.0000	100.0000	V_{G100}	1.0500	1.0390			
P_{G77}	99.9802	100.0000	V_{G103}	1.0499	1.0389			
P_{G80}	576.9999	539.4892	V_{G104}	1.0411	1.0368			
P_{G85}	99.9999	100.0000	V_{G105}	1.0404	1.0390			
P_{G87}	23.2224	24.9167	V_{G107}	1.0500	1.0389			
P_{G89}	205.0435	211.1767	V_{G110}	1.0438	1.0382			
P_{G90}	100.0000	100.0000	V_{G111}	1.0491	1.0389			
P_{G91}	81.3704	81.1335	V_{G112}	1.0476	1.0385			
P_{G92}	99.9999	100.0000	V_{G113}	1.0413	1.0263			
P_{G99}	71.0863	62.3132	V_{G116}	1.0386	1.0294			
P_{G100}	196.0375	192.3381	$T1$	1.0271	1.0334	Tap transformers : p.u		
P_{G103}	34.1073	34.0896	$T2$	1.0011	1.0072			
P_{G104}	56.4902	56.4438	$T3$	1.0011	1.0072			
P_{G105}	95.9247	95.8767	$T4$	0.9750	0.9809			
P_{G107}	85.7417	85.6577	$T5$	1.0011	1.0072			
P_{G110}	66.7786	66.7212	$T6$	1.0271	1.0334			
P_{G111}	0.2352	0.1494	$T7$	0.9750	0.9809			
P_{G112}	99.9855	99.9977	$T8$	0.9750	0.9809			
P_{G113}	72.9385	73.9359	$T9$	0.9750	0.9809			
P_{G116}	99.9999	99.9999	$Qc5$	0	−78.8953	Reactive power of shunt SVC exchanged with the network (MVAR)		
V_{G1}	1.0003	0.9861	$Qc34$	0	27.6133			
V_{G4}	1.0309	1.0179	$Qc37$	0	−49.3095			
V_{G6}	1.0289	1.0159	$Qc44$	0	19.7238			
V_{G8}	1.0335	1.0253	$Qc45$	0	19.7238			
V_{G10}	1.0277	1.0142	$Qc46$	0	19.7238			
V_{G12}	1.0260	1.0142	$Qc48$	0	9.8619			
V_{G15}	1.0271	1.0107	$Qc74$	0	23.6686			
V_{G18}	1.0345	1.0182	$Qc79$	0	39.4476			
V_{G19}	1.0291	1.0126	$Qc82$	0	39.4476			
V_{G24}	1.0500	1.0362	$Qc83$	0	19.7238			
Ploss (MW)				38.4761	37.2839			
VD (p.u)				**1.5116**	**1.0520**			
LF (p.u)				**1.485**	**1.485**			

The bold values indicate the best results found using the proposed algorithm

contingency. Results found using the interactive SCA are competitive in terms of solution quality and convergence characteristics compared to the standard algorithm and to other recent methods. In the future and due to the efficient performances of the proposed power system planning strategy based interactive SCA, the authors will strive to adapt and apply the proposed algorithm for solving the dynamic OPF considering the ramp down and ramp up for large power system under critical situations considering the integration and coordination between different types of FACTS devices and renewable sources.

References

1. Carpentier J (1962) Contribution ‘a l“etude du Dispatching Economique (Contribution to the study of economic dispatch). Bull Soc Fr Elect 3:431–447

2. Dommel HW, Tinney TF (1968) Optimal power flow solutions. IEEE Trans Power Appar Syst 87(5):1866e76
3. Mota-Palomino R, Quintana VH (1986) Sparse reactive power scheduling by a penalty-function linear programming technique. IEEE Trans Power Syst 1(3):31–39
4. Alsac O, Scott B (1974) Optimal load flow with steady state security. IEEE Trans Power Appar Syst PAS-93(3):745–751
5. Burchett RC, Happ HH, Vierath DR (1984) Quadratically convergent optimal power flow. IEEE Trans Power Appar Syst 103(11):3267–3276
6. Sun DI, Ashley B, Brewer B, Hughes A, Tinney WF (1984) Optimal power flow by Newton approach. IEEE Trans Power Appar Syst 103(10):2864–2875
7. Yan X, Quintana VH (1999) Improving an interior point based OPF by dynamic adjustments of step sizes and tolerances. IEEE Trans Power Syst 14(2):709–717
8. Frank S, Steponavice I, Rebennak S (2012) Optimal power flow: a bibliographic survey I, formulations and deterministic methods. Int J Energy Syst 3(3):221–258
9. Frank S, Steponavice I (2012) Optimal power flow: a bibliographic survey II. Non-deterministic and hybrid methods, Energy Syst. 3(3):259–289
10. Capitanescu F (2016) Critical review of recent advances and further developments needed in AC optimal power flow. Electr Power Syst Res 136:57–68
11. Mirjalili S, Mirjalili SM, Lewis A (2014) Grey wolf optimizer. Adv Eng Softw 69:46–61
12. Mahdad B, Srairi K (2015) Blackout risk prevention in a smart grid based flexible optimal strategy using Grey Wolf-pattern search algorithms. Energy Convers Manag 98:411–429
13. Sulaiman MH, Mustaffa Z, Mohamed MR, Aliman O (2015) Using the gray wolf optimizer for solving optimal reactive power dispatch problem. Appl Soft Comput 32:286–292
14. Jangir P, Parmar SA, Trivedi IN, Bhesdadiya RH (2017) A novel hybrid Particle Swarm Optimizer with multi verse optimizer for global numerical optimization and optimal reactive power dispatch problem. Eng Sci Technol Int J 20(2):570–586
15. Panda A, Tripathy M (2015) Security constrained optimal power flow solution of wind-thermal generation system using modified bacteria foraging algorithm. Energy 93:816–827
16. Pandiarajan K, Babulal CK (2016) Fuzzy harmony search algorithm based optimal power flow for power system security enhancement. Int J Electr Power Energy Syst 78:72–79
17. Mahdad B, Srairi k (2016) Security constrained optimal power flow solution using new adaptive partitioning flower pollination algorithm. Appl Soft Comput 46:501–522
18. Othman MM, El-Khattam W, Hegazy YG, Abdelaziz AY (2016) Optimal placement and sizing of voltage controlled distributed generators in unbalanced distribution networks using supervised firefly algorithm. Electr Power Energy Syst 82:105–113
19. Duman S (2016) Symbiotic organisms search algorithm for optimal power flow problem based on valve-point effect and prohibited zones. Neural Comput Appl 1–15. doi:10.1007/s00521-016-2265-0
20. Abaci K, Yamacli V (2016) Differential search algorithm for solving multi-objective optimal power flow problem. Electr Power Energy Syst 79:1–10
21. Mohamed A-AA, Mohamed YS, El-Gaafary AAM, Hemeid AM (2017) Optimal power flow using moth swarm algorithm. Electr Power Syst Res 142:190–206
22. Singh RP, Mukherjee V, Ghoshal SP (2016) Particle swarm optimization with an aging leader and challengers algorithm for the solution of optimal power flow problem. Appl Soft Comput 40:161–177
23. Xu Y, Yang H, Zhang R, Dong ZY, Lai M, Wong KP (2016) A contingency partitioning approach for preventive–corrective security-constrained optimal power flow computation. Electr Power Syst Res 132:132–140
24. Kumar AR, Premalath L (2015) Optimal power flow for a deregulated power system using adaptive real coded biogeography-based optimization. Electr Power Energy Syst 73:393–399
25. Radosavljevic' J, Jevtic' M, Milovanovic' M (2016) A solution to the ORPD problem and critical analysis of the results. Electr Eng. doi:10.1007/s00202-016-0503-1
26. Roberge V, Tarbouchi M, Okou F (2016) Optimal power flow based on parallel metaheuristics for graphics processing units. Electr Power Syst Res 140:344–353
27. Mirjalili S (2016) SCA: a sine cosine algorithm for solving optimization problems. Knowl Based Syst 96:120–133
28. Kessel P, Glavitsch H (1986) Estimating the voltage stability of a power system. IEEE Trans Power Deliv 1:346–354. doi:10.1109/TPWRD.1986.4308013
29. Zimmerman RD, Murillo-Sánchez CE, Thomas RJ (2011) MATPOWER: steady-state operations, planning and analysis tools for power systems research and education. IEEE Trans Power Syst 26(1):12–19